Check for updates

Differences in the choroid plexus volume and microstructure are associated with body adiposity

Joseph S. R. Alisch, Josephine M. Egan
and Mustapha Bouhrara*

Laboratory of Clinical Investigation, National Institute on Aging, National Institutes of Health,
Baltimore, MD, United States

The choroid plexus (CP) is a cerebral structure located in the ventricles that functions in producing most of the brain's cerebrospinal fluid (CSF) and transporting proteins and immune cells. Alterations in CP structure and function has been implicated in several pathologies including aging, multiple sclerosis, Alzheimer's disease, and stroke. However, identification of changes in the CP remains poorly characterized in obesity, one of the main risk factors of neurodegeneration, including in the absence of frank central nervous system alterations. Our goal here was to characterize the association between obesity, measured by the body mass index (BMI) or waist circumference (WC) metrics, and CP microstructure and volume, assessed using advanced magnetic resonance imaging (MRI) methodology. This cross-sectional study was performed in the clinical unit of the National Institute on Aging and included a participant population of 123 cognitively unimpaired individuals spanning the age range of 22 − 94 years. Automated segmentation methods from FreeSurfer were used to identify the CP structure. Our analysis included volumetric measurements, quantitative relaxometry measures (T_1 and T_2), and the diffusion tensor imaging (DTI) measure of mean diffusivity (MD). Strong positive associations were observed between WC and all MRI metrics, as well as CP volume. When comparing groups based on the established cutoff point by the National Institutes of Health for WC, a modest difference in MD and a significant difference in T_1 values were observed between obese and lean individuals. We also found differences in T1 and MD between obese and overweight individuals as defined using the BMI cutoff. We conjecture that these observations in CP volume and microstructure are due to obesity-induced inflammation, diet, or, very likely, dysregulations in leptin binding and transport. These findings demonstrate that obesity is strongly associated with a decline in CP microstructural integrity. We expect that this work will lay the foundation for further investigations on obesity-induced alterations in CP structure and function.

Introduction

Obesity, which is characterized by excessive adipose tissue, is a complex disease that impacts several physiological systems of the body. It also renders people at increased risk for an array of other diseases including, but not limited to, diabetes, cardiovascular diseases and cancer—all of which drastically increase the global health burden of this condition (1, 2). Many lines of research have also provided support for an association between obesity and several central nervous system (CNS) pathologies such as Alzheimer's disease (3, 4) and multiple sclerosis (5, 6). Obesity is understood to enact a variety of down-stream effects in the CNS through decreased myelin content (7), and effects on cortical thickness (8), gray matter volume (9) and cerebral blood flow (10). Further, a common feature for many of these neurodegenerative processes is inflammation, which is attenuated by exercise and, not surprisingly, dietary interventions (11, 12).

Implicated in mediating the neuroinflammatory effects of obesity is the choroid plexus (CP) (13–15), a critical cerebral structure necessary for cerebrospinal fluid (CSF) production. The CP is housed in the ventricles, which are a network of four communicating cavities responsible for providing protection and circulating CSF to the brain. Structurally, the CP consists of a single layer of cuboidal epithelial cells connected by apical tight junctions that interfaces CSF and fenestrated capillaries forming the blood-CSF barrier (BCSFB) (16). Moreover, the CP has various other functions such as strict regulation of transport systems that modulate CSF composition by allowing passage of nutrients such as glucose, lipids and proteins, solutes and inflammatory cells (16), as well as producing growth factors and hormones involved with development and maintenance of brain function (17). Previous research has shown that dysfunction of the CP and ventriculomegaly are involved in the pathogenesis of neurodegenerative diseases including Alzheimer's disease (18–20) and multiple sclerosis (21–23). Additionally, diet formulations in studies that contain high fat and cholesterol rich content have been suggested to contribute to these pathological features (14, 24, 25).

Several methods used in identifying CP structure and lateral ventricles (LV) include magnetic resonance imaging (MRI) quantitative techniques (26). Current works that have evaluated the CP *in-vivo* used volumetric analyses, relaxometry, specifically longitudinal and transverse relaxation times (T_1 and T_2), and mean diffusivity (MD) derived from diffusion tensor imaging (DTI), to assess CP volume and microstructure (27–32). T_1 and T_2 both depend on macromolecular tissue composition as well as water mobility. Thus, observed changes in T_1 or T_2 are directly associated with cerebral microstructural tissue changes (33). Similarly, MD can also be used to identify cerebral tissue microstructural integrity based on water content and mobility (34, 35). These previous MRI-based studies have shown that the CP and LV significantly

increase in volume during disease states and normative aging (28–32). Moreover, the CP exhibits increases in T_1, T_2 and MD during normative aging, reflecting increased water mobility that suggests a decrease in microstructural integrity (27, 28). In a cross-sectional study that looked at obesity in Alzheimer's disease patients, Ho and colleagues found that after performing a T_1-weighted imaging volumetric analysis, cerebral ventricular enlargement was associated with a high body mass index (BMI) after controlling for age, sex, and education (36). The authors conjectured that a high BMI could result in different outcomes in brain volume measurements. In another study that looked at the relationship between allostatic load and CP volume that was measured from T_1-weighted imaging, the authors found a positive association in individuals with schizophrenia (37). Briefly, allostatic load represents the culmination of chronic stress and is a combined measure of cardiovascular indicators, metabolic indicators including BMI and waist circumference (WC), inflammation, and neuroendocrine hormones (37). While not specific to obesity, previous studies have shown an association between obesity and high allostatic load due to several factors such as diet, systemic inflammation, and other lifestyle and environmental characteristics (38). Despite the current available literature, no MRI study, to our knowledge, has examined the microstructural impact of obesity on the CP in the absence of a major CNS pathology.

In this study, our participant population included 123 cognitively unimpaired subjects with healthy weight, overweight, or obesity over the age range of 22 – 94 years. Our main goal was to elucidate the relationship between LV volume, CP volume, and CP microstructure, which was assessed using T_1, T_2 or MD, and BMI or WC, as measures of obesity. Here, we lay the groundwork in our understanding of CP and LV-specific changes related to metabolic dysfunction, specially, obesity.

Materials and methods

Participants

Experimental procedures were performed in compliance with our local Institutional Review Board, and participants provided written informed consent. Participants were drawn from the Baltimore Longitudinal Study of Aging (BLSA) (39, 40), and the Genetic and Epigenetic Signatures of Translational Aging Laboratory Testing (GESTALT) study. The study populations, experimental design, and measurement protocols of the BLSA have been previously reported (39, 40). The goal of the BLSA and GESTALT studies is to evaluate multiple biomarkers related to aging. We note that the inclusion and exclusion criteria for these two studies are essentially identical. Participants underwent testing at the National Institute on Aging's clinical research unit and were excluded if they had

metallic implants, neurologic, or medical disorders. Further, all participants underwent a battery of cognitive tests and participants with cognitive impairment were excluded (41).

MR imaging

We emphasize that all MRI studies and ancillary measurements were performed with the same MRI system, running the same pulse sequences, at the same facility, and directed by the same investigators for both BLSA and GESTALT participants. The MRI protocol was approved by the MedStar Research Institute and the National Institutes of Health Intramural Ethics Committees, and all examinations were performed in compliance with the standards established by the National Institutes of Health Institutional Review Board. MRI scans were performed on a 3T whole body Philips MRI system (Achieva, Best, The Netherlands) using the internal quadrature body coil for transmission and an eight-channel phased-array head coil for reception. For each participant, the T_1 and T_2 maps were derived from 3D spoiled gradient recalled echo (SPGR) images were acquired with flip angles of [2 4 6 8 10 12 14 16 18 20]°, echo time (TE) of 1.37 ms, repetition time (TR) of 5 ms, and acquisition time of ~5 min, as well as 3D balanced steady state free precession (bSSFP) images acquired with flip angles of [2 4 7 11 16 24 32 40 50 60]°, TE of 2.8 ms, TR of 5.8 ms, and acquisition time of ~6 min. The bSSFP images were acquired with radiofrequency excitation pulse phase increments of 0 or π in order to account for off-resonance effects (42–45). All SPGR and bSSFP images were acquired with an acquisition matrix of 150 × 130 × 94, voxel size of 1.6 mm × 1.6 mm × 1.6 mm. Further, we used the double-angle method (DAM) to correct for excitation radio frequency inhomogeneity (46). For this, two fast spin-echo images were acquired with flip angles of 45° and 90°, TE of 102 ms, TR of 3000 ms, acquisition voxel size of 2.6 mm × 2.6 mm × 4 mm, and acquisition time of ~4 min. All images were acquired with field of view (FoV) of 240 mm × 208 mm × 150 mm. The total acquisition time was ~21 min. Finally, the MD map was derived from the DTI dataset. The DTI protocol consisted of diffusion-weighted images (DWI) acquired with single-shot EPI, TR of 10,000 ms, TE of 70 ms, two b-values of 0 and 700 s/mm^2, with the latter encoded in 32 directions, acquisition matrix of 120 × 104 × 75, and acquisition voxel size of 2 mm × 2 mm × 2 mm. Images were acquired with FoV of 240 mm × 208 mm × 150 mm. All images were reconstructed to a voxel size of 1 mm × 1 mm × 1 mm.

Image processing

CP and LV volumes calculation: for each participant, corresponding T_1-weighted SPGR images were used. Specifically, the FreeSurfer Aseg Atlas (47) was nonlinearly

registered to the SPGR images averaged over all flip angles using the cortical reconstruction (recon-all) pipeline from the Freesurfer v7.1.1 software[1] (48) (Figure 1). Volumetric measurements were then extracted from the CP and LV regions of interest (ROIs). This method has been used in several other studies indicating reliable CP and LV segmentation (28–30, 32, 34, 49, 50). All CP and LV ROIs were thoroughly examined and corrected manually when needed.

T_1 and T_2 mapping: using the FMRIB Software Library (FSL) software (51), all SPGR, bSSFP, and DAM images were linearly registered to the SPGR image acquired at a flip angle of 8° and the derived transformation matrix was then applied to the original SPGR, bSSFP, and DAM images. Next, a whole-brain T_1 map was generated from the co-registered SPGR dataset using the DESPOT1 analysis and assuming a single relaxing component using the stochastic regions contraction (SRC) algorithm while correcting for transmit field, B_1, inhomogeneities (52, 53). The B_1 map was generated from the co-registered fast spin-echo using the DAM approach (46). Further, using these derived T_1 and B_1 maps as input parameters, a whole-brain T_2 map was generated from the co-registered bSSFP dataset using the DESPOT2 analysis and assuming a single component using the SRC algorithm (52, 53). B_1, T_1, and T_2 maps were generated using in-house MATLAB scripts. All these MATLAB codes are available upon request. Next, using FreeSurfer, the SPGR image averaged over all flip angles for each participant was registered using nonlinear registration to FreeSurfer's Aseg atlas and the derived transformation matrix was then applied to the corresponding T_1 and T_2 maps. Finally, the mean T_1 and T_2 values in the CP ROI were calculated. We note that 10 datasets were excluded from the subsequent analyses due to issues with the imaging data including motion artefacts.

MD mapping: the DW images were corrected for eddy current and motion effects using affine registration tools implemented in FSL (51), and registered to the DW image obtained with b = 0 s/mm^2. Moreover, whole-brain MD map was derived from the co-registered DWI data. We used the DTIfit tool implemented in FSL to calculate the eigenvalue maps which were used to calculate MD (54). Finally, for each participant, the DW image obtained at b = 0 s/mm^2 was nonlinearly registered to FreeSurfer's Aseg atlas and the calculated matrix of transformation was then applied to the corresponding MD map. Finally, the mean MD value in the CP ROI was calculated. We note that 8 datasets were excluded from the subsequent analyses due to issues with the imaging data including motion artefacts.

---

1 https://surfer.nmr.mgh.harvard.edu/

Statistical analysis

For each ROI, the correlation between BMI or WC and CP volume, LV volume, T_1, T_2, or MD was investigated using multiple linear regression with the mean CP volume, LV volume, T_1, T_2, or MD value within the ROI as the dependent variable and BMI or WC, sex, ethnicity, age, and age^2 as independent variables, after mean age centering. The inclusion of age^2 as an independent variable is based on our and others' recent observations that cerebral maturation follows a quadratic relationship with age (55, 56). We note that the CP and LV volumes were corrected for the total intracranial volume (ICV). Further, given the potential correlation between the CP volume and the LV volume, the association between the CP volume and BMI or WC was also conducted while accounting for the LV volume.

To investigate the associations between BMI or WC and CP volume, LV volume, T_1, T_2, or MD between the groups of subjects with healthy weight (lean), overweight, and obesity, we performed between-group ANCOVA analyses for each ROI. These included i) obese vs. lean groups, ii) overweight vs. lean groups, and iii) obese vs. overweight groups. All between-group comparisons controlled for sex, ethnicity, age and age^2.

Finally, to explore the potential effect of partial volume on the association between T_1, T_2, or MD and BMI or WC due to contamination from CSF, we calculated mean values of these MR parameters in the ventricular CSF regions and conducted a regression analysis accounting for the confounding variable as described above. CSF maps were generated using FSL FAST segmentation (57).

The threshold for statistical significance was set to $p < 0.05$. Given the exploratory nature of this study and concerns about type 2 error, all analyses were conducted without correction for multiple comparison. Calculations were performed with MATLAB (MathWorks, Natick, MA, USA). All MATLAB codes are available upon request from the corresponding author.

Results

The final cohort consisted of 123 cognitively unimpaired volunteers ranging in age from 21 to 94 years (55.0 ± 20.5 years) of which 65 were men (56.0 ± 21.5 years) and 58 were women (54.0 ± 19.6 years), after exclusion of nine participants with cognitive impairment (Table 1). Age ($p > 0.1$) did not differ significantly between men and women. The number of participants per age-decade was: 14 (7 females) within 20-29 years, 17 (6 females) within 30-39 years, 35 (20 females) within 40-49 years, 8 (3 females) within 50-59 years, 9 (6 females) within 60-69 years, 17 (7 females) within 70-79 years, 21 (9 females) within 80-89 years, and 2 (0 females) within 90-99 years. Following established BMI cutoff points (58), the cohort consisted of 56 lean participants (BMI < 25), 50 overweight

participants (25 ≤ BMI < 30), and 17 participants with obesity (BMI ≥ 30), while following the National Institutes of Health cutoff points for WC, the cohort consisted of 71 lean participants (WC < 94 cm for men and WC < 80 cm for women), 31 overweight participants (94 ≤ WC < 102 for men and 80 ≤ WC < 88 for women), and 21 participants with obesity (WC ≥ 102 for men and WC ≥ 88 for women). Finally, we note that BMI and WC exhibited a modest correlation leading to a coefficient of correlation value of $R^2 = 0.54$.

Figure 2 shows regression relationships between the CP volume, LV volume, after correcting for the total intracranial volume, T_1, T_2, or MD and BMI, after adjusting for sex, ethnicity, age, and age^2. Visual inspection indicates that higher BMI values corresponds to higher CP volume, LV volume, T_1, T_2, or MD values. Accounting for the LV volume in the regression of CP vs BMI or WC had a marginal effect. Further, the multiple regression analysis indicates that the correlation between the LV volume or T_1 and BMI was statistically significant ($p_{BMI} < 0.05$) or close to significance ($p_{BMI} < 0.1$) (Figure 2; Table 2). Furthermore, as expected, a statistically significant age effect was found for all MR metrics evaluated (Figure 3; Table 2). Similarly, the quadratic effect of age, age^2, was statistically significant or close to significance for most metrics (Figure 3; Table 2). Additionally, the correlation between CP volume or MD and sex was found to be statistically significant (Table 2).

Figure 4 shows regression relationships between the CP volume, LV volume, T_1, T_2, or MD and WC, after adjusting for sex, ethnicity, age, and age^2. Visual inspection indicates that larger WC corresponds to higher CP volume, LV volume, T_1, T_2, or MD values. Further, the multiple regression analysis indicates that this correlation between the LV volume or T_1 and WC was statistically significant ($p_{WC} < 0.05$) or close to significance ($p_{WC} < 0.1$) (Table 3). Furthermore, as expected, a statistically significant age effect was found for all metrics evaluated (Table 3). Moreover, the quadratic effect of age, age^2, was statistically significant for most MR metrics (Table 3). Additionally, the correlation between CP volume or MD and sex was found to be statistically significant (Table 3).

Table 4 shows demographic characteristics of the lean, overweight and obese subgroups stratified using the established BMI or WC cutoff points. While using the BMI cutoff point both the lean and overweight group incorporated a similar number of participants, the number of overweight participants decreased substantially when the WC cutoff point is used. In all case, the obese groups incorporated a much lower number of participants. There were no statistically significant differences in MMSE between groups for both cutoff points. Table 5 summarizes the results of the between-group ANCOVA analyses of the associations between BMI or WC and CP volume, LV volume, T_1, T_2, or MD. In comparing subjects with obesity to lean subjects, we found higher CP volume, LV volume, T_1, T_2 or MD in the group of subjects with obesity despite controlling for age, age^2, sex, and ethnicity as well as LV volume for the CP volume analysis. This effect was significant for LV and T1,and
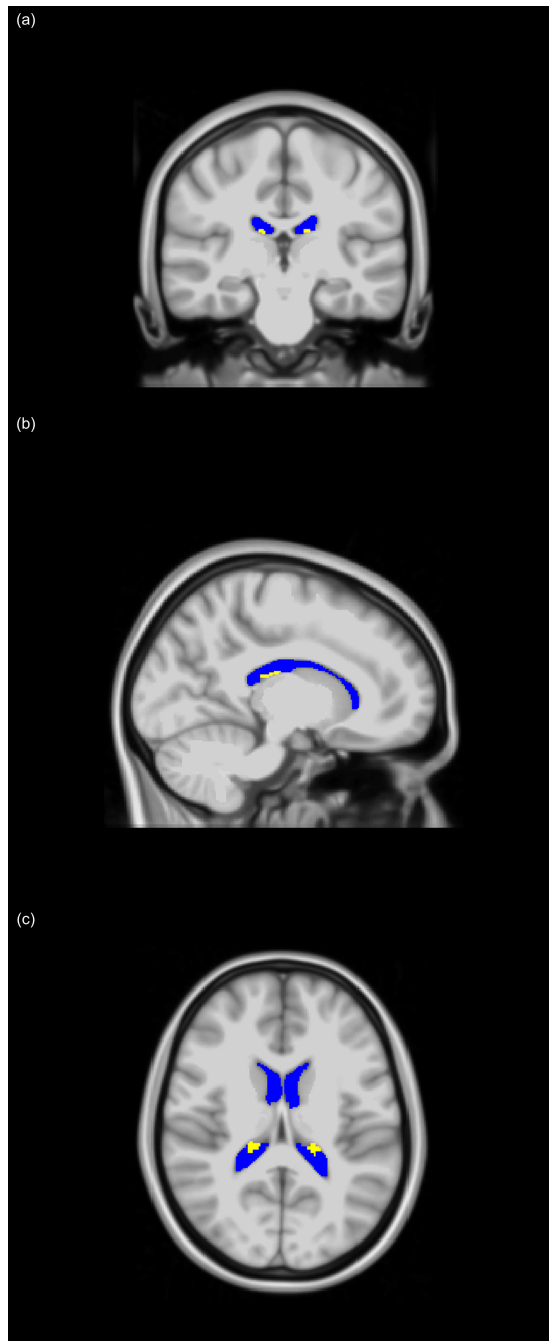
FIGURE 1
Choroid plexus (CP - yellow) and lateral ventricles (LV - blue) regions of interest (ROIs), extracted using FreeSurfer and projected on the MNI atlas for three different views: **(A)** coronal, **(B)** sagittal, and **(C)** axial. All images are in radiological convention.

we found higher CP volume, LV volume, T_1, T_2, or MD in the overweight group as compared to the lean group. Finally, in comparing subjects with obesity to overweight subjects as defined by BMI, we found significantly higher T_1 and MD in the group of subjects with obesity, with both groups defined by either BMI or WC exhibiting higher CP volume, LV volume, T_1, T_2, or MD values in the subjects with obesity as compared to overweight subjects. The mean and standard deviation values of each MRI metric for each group are provided in Table 6.

Further, it is readily seen that all MR parameters derived from the CSF exhibit a flat fitting line indicating no associations with BMI or WC (Figure 5). Our statistical analysis indicated that BMI and WC exhibited nonsignificant associations ($p > 0.1$) with each of the MR parameters of T_1, T_2 and MD.

Discussion

In this study, we provided the first report of an association between obesity and structural alterations in the CP using MR volumetry, quantitative relaxometry and DTI. When comparing groups of lean, overweight and obese stratified using the established cutoff points for WC (58), we found a modest difference in MD values and a significant difference in T_1 values between obese and lean participants after correcting for age, sex and ethnicity, with MD and T_1 exhibiting higher values with WC. Stratification by the BMI cutoff revealed significant differences in T1 and MD between obese and overweight individuals. Briefly, MD describes the overall diffusion and motion of water molecules in the brain (35, 59), while T_1 describes the rate at which excited protons return to equilibrium and also depends on water content and mobility (33). For both of these MRI metrics, higher values reflect more water mobility or microstructural tissue deterioration. Therefore, the presence of increased water mobility in obese participants may be indicative of decreased microstructural integrity in the CP. We provisionally attribute this observation to dysregulations in leptin binding, which is a characteristic feature of obesity (60). Indeed, leptin is an adipocyte-derived hormone encoded by the obesity (*ob*) gene that regulates many physiological processes including energy homeostasis, appetite and immune function (61). The CP is one of the main access points by which leptin enters the CNS. Transport across the CP epithelium is regulated by the leptin receptors, which includes the highly expressed short form (Ob-Ra) and a long form (Ob-Rb), and megalin (LRP2) (62–64). In one study that examined the neuropathology of BTBR *ob/ob* mice, a model of leptin deficiency, the CP underwent ultrastructural remodeling, specifically atypical vacuolization and vesiculation of the basilar infoldings of the epithelial cells lining the LV. The authors concluded that this could represent a dysfunctional CP with abnormalities in leptin signaling (65).

close to statistical significance for MD. Moreover, controlling for these same covariates, while comparison of overweight to lean subjects as defined by BMI or WC did not show statistically significant differences in CP volume, LV volume, T_1, T_2, or MD,

TABLE 1 Demographic characteristics of participants.

Participant Demographics	Total Sample (N = 123)
Age (yrs.): mean ± SD *(min – max)*	56.2 ± 20.9 *(22-94)*
Sex	
Men	65 *(52.8%)*
Women	58 *(47.2%)*
MMSE	28.8 ± 1.4 *(25-30)*
BMI (Kg/m^2): mean ± SD *(min – max)*	25.8 ± 3.6 *(18.3-35.8)*
WC (cm): mean ± SD *(min – max)*	86.9 ± 10.4 *(63.0-112.8)*

SD, standard deviation; min, minimum; max, maximum; MMSE, Mini-Mental State Examination; BMI, body-mass index; WC, waist circumference. Italic indicates the percentage or range of the variable.

In addition to ultrastructural remodeling, a compromised BCSFB has been implicated with obesity. One report showed that CSF/serum albumin ratio (QAlb), a biomarker of BCSFB permeability (66), was positively associated with both BMI and WC (67). A higher QAlb indicates higher permeability and is suggestive of damage to structures that function as barriers. Finally, in an animal study of diet-induced obesity, it has been found that consumption of a high energy diet decreased expression of tight junction proteins in the CP, thus compromising its structural integrity (14). However, increased water movement in the CP could also be due to increased cerebrospinal fluid secretion. Indeed, the CP secretes CSF and partially determines intracranial pressure (ICP). Mounting evidence, from preclinical and clinical investigations, have shown that obesity increases ICP which may lead to increased ventricular volume with obesity (68, 69), as observed here. Further histological investigations are required to shed the light on these aspects relating obesity to the CP's microstructural differences.

FIGURE 2
Regression results for the relationship between the lateral ventricle (LV) volume/intracranial volume (ICV), T_1, T_2, or mean diffusivity (MD) and body mass index (BMI) adjusted for age, age^2, sex, and ethnicity. For the choroid plexus (CP) volume/ICV, regression results were controlled for age, age^2, sex, ethnicity, and LV volume. The coefficient of determination, R^2, and p-value, p, of the multiple linear regression model are reported. The CP volume, LV volume, T_1, T_2, or MD exhibited significant positive correlations with BMI.
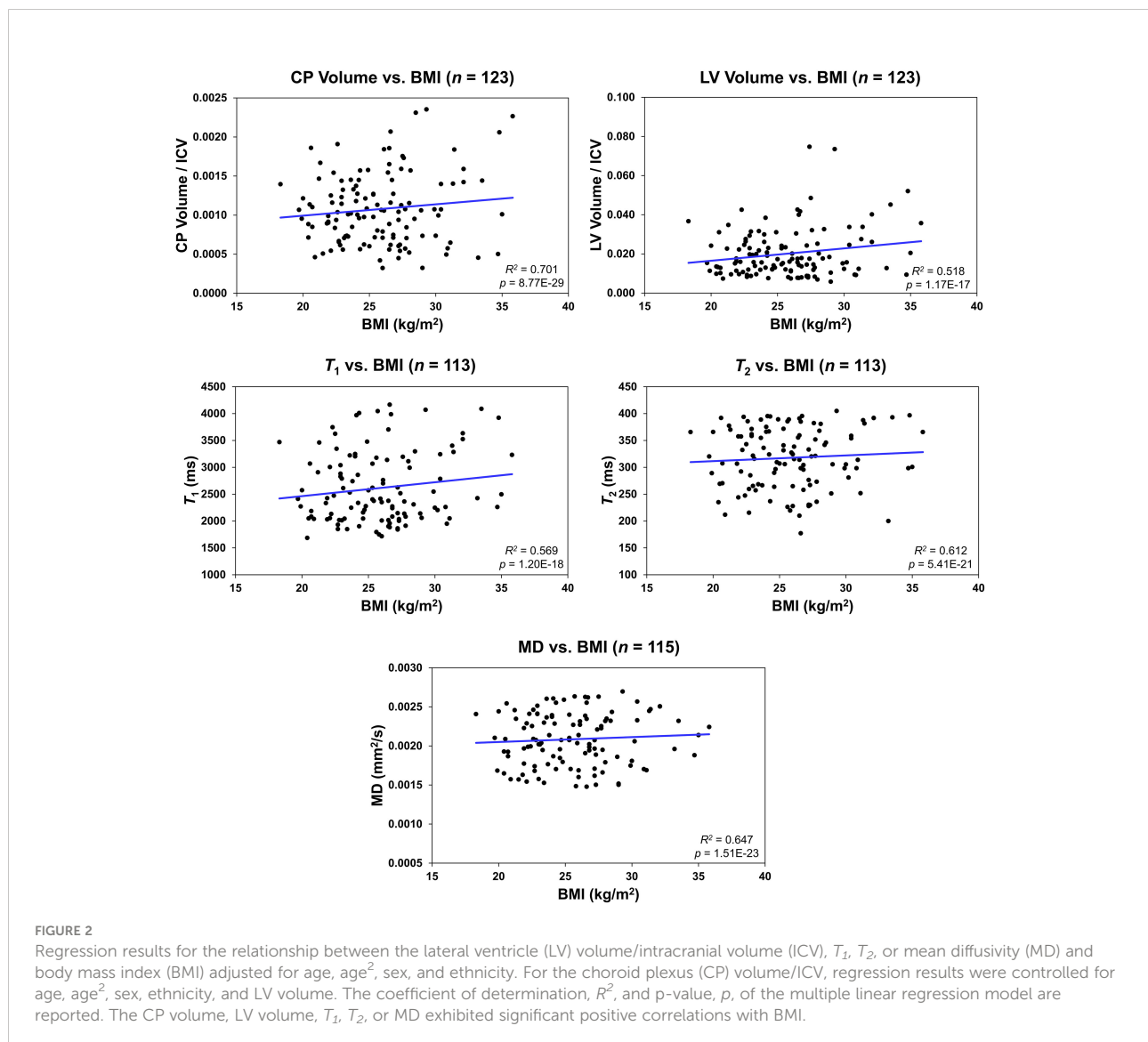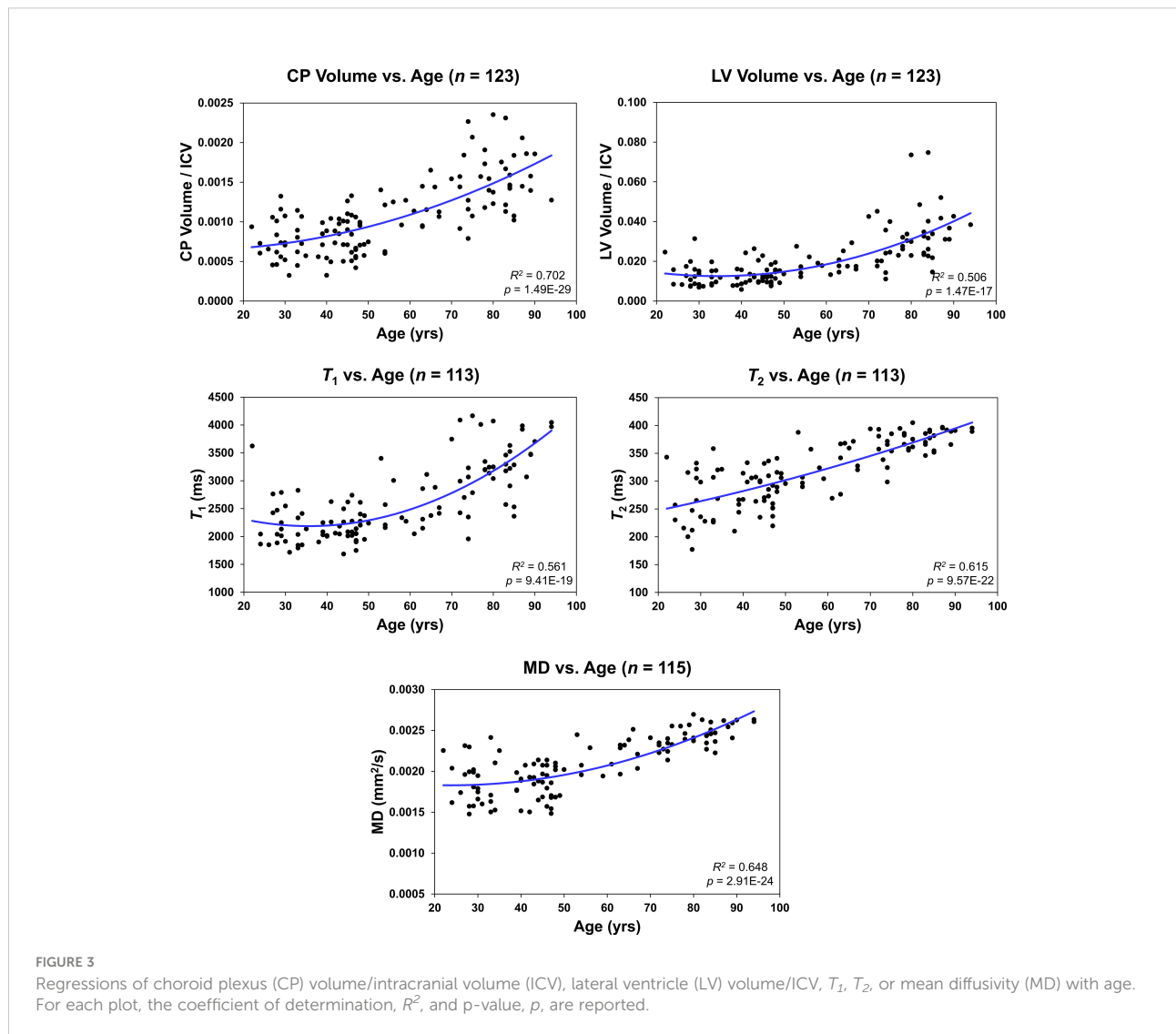
TABLE 2 Slope, β, and significance, p, of the regression terms incorporated in the multiple linear regression given by: Lateral ventricle (LV) volume/intracranial volume (ICV), T_1, T_2, or mean diffusivity (MD) $\sim \beta_0 + \beta_{BMI} \times$ BMI $+ \beta_{age} \times$ age $+ \beta_{age}^2 \times$ age$^2 + \beta_{sex} \times$ sex $+ \beta_{ethnicity} \times$ ethnicity.

	Age		Age^2		Sex		Ethnicity		BMI	
	β_{age}	p_{age}	β_{age}^2	p_{age}^2	β_{sex}	p_{sex}	$\beta_{ethnicity}$	$p_{ethnicity}$	β_{BMI}	p_{BMI}
CP volume/ICV	7.39×10^{-6}	$\mathbf{2.56 \times 10^{-6}}$	-4.99×10^{-8}	0.49	1.01×10^{-4}	**0.03**	-2.84×10^{-5}	0.70	-4.28×10^{-6}	0.51
LV volume/ICV	3.56×10^{-4}	$\mathbf{1.82 \times 10^{-14}}$	9.17×10^{-6}	$\mathbf{1.75 \times 10^{-4}}$	1.45×10^{-4}	0.93	-1.51×10^{-3}	0.55	4.43×10^{-4}	$\mathbf{4.77 \times 10^{-2}}$
T_1	20.20	$\mathbf{6.63 \times 10^{-17}}$	0.52	$\mathbf{2.54 \times 10^{-5}}$	18.21	0.83	-61.85	0.66	20.25	**0.07**
T_2	2.08	$\mathbf{1.46 \times 10^{-22}}$	9.29×10^{-3}	0.34	-2.43	0.72	-16.69	0.15	0.48	0.61
MD	1.13×10^{-5}	$\mathbf{9.67 \times 10^{-21}}$	1.57×10^{-7}	$\mathbf{4.82 \times 10^{-3}}$	1.02×10^{-4}	$\mathbf{8.93 \times 10^{-3}}$	2.10×10^{-6}	0.97	4.09×10^{-6}	0.45

For the choroid plexus (CP) volume, the multiple linear regression model includes the LV volume as an additional covariate given by CP volume/ICV $\sim \beta_0 + \beta_{BMI} \times$ BMI $+ \beta_{age} \times$ age $+ \beta_{age}^2 \times$ age$^2 + \beta_{sex} \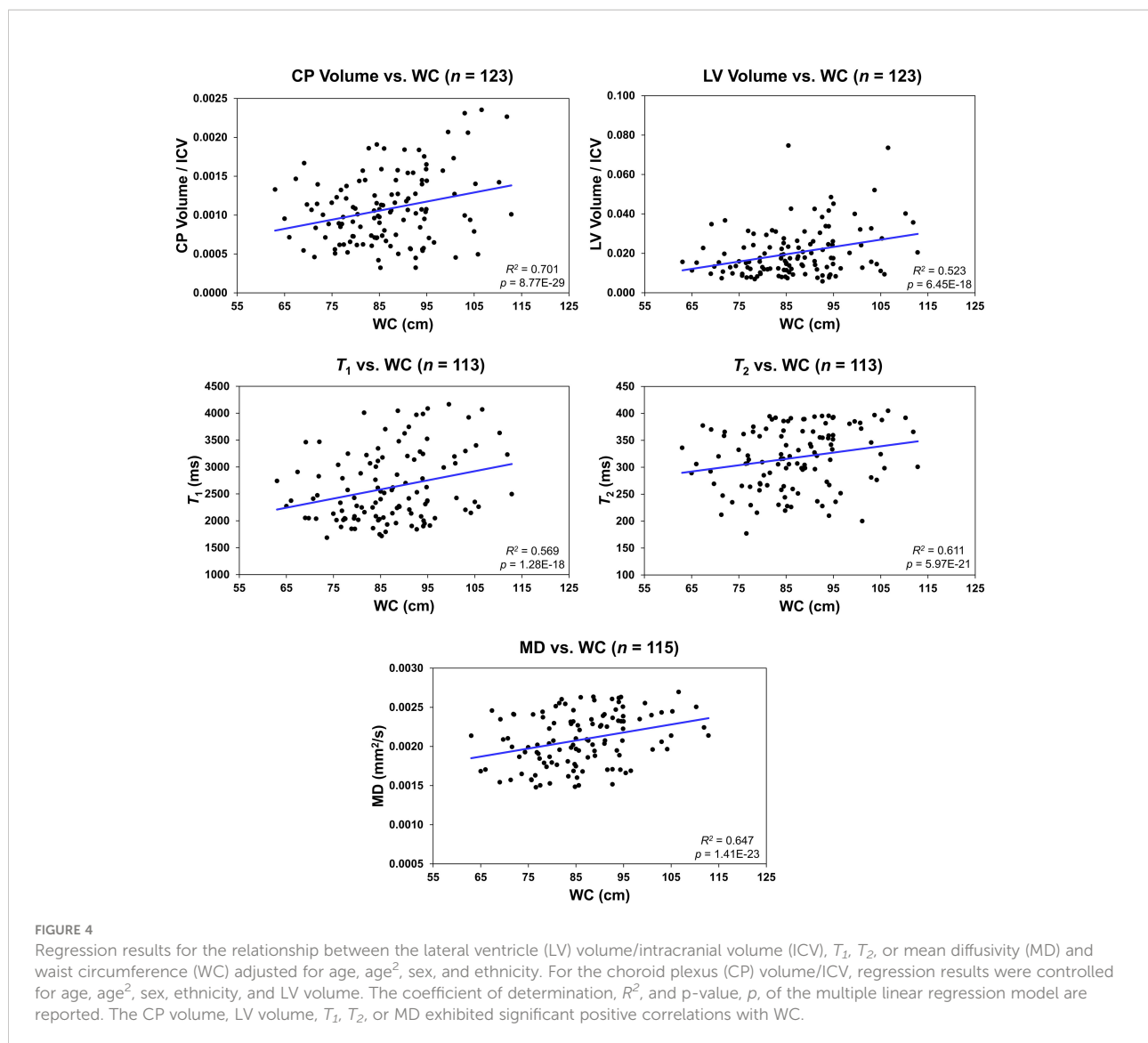times$ sex $+ \beta_{ethnicity} \times$ ethnicity $+ \beta_{LV} \times$ LV. Sex and ethnicity results are not shown for associations with CP volume, LV volume, T_1, T_2, or MD. Bold indicates significance (p < 0.05) or close to significance (p < 0.1).

Positive associations were also observed between obesity, measured either by BMI or WC, and CP volume, but did not have as strong of an effect as age. Previous research has shown that CP volume increases during pathological states such as stroke (30), multiple sclerosis (31) and Alzheimer's disease (70), where neuro-inflammation is one of many characteristic features of these diseases. Obesity causes increasing inflammation in the CNS (15), as well as an increase in circulating serum leptin. In fact, one study

FIGURE 3
Regressions of choroid plexus (CP) volume/intracranial volume (ICV), lateral ventricle (LV) volume/ICV, T_1, T_2, or mean diffusivity (MD) with age. For each plot, the coefficient of determination, R^2, and p-value, p, are reported.

FIGURE 4

Regression results for the relationship between the lateral ventricle (LV) volume/intracranial volume (ICV), T_1, T_2, or mean diffusivity (MD) and waist circumference (WC) adjusted for age, age^2, sex, and ethnicity. For the choroid plexus (CP) volume/ICV, regression results were controlled for age, age^2, sex, ethnicity, and LV volume. The coefficient of determination, R^2, and p-value, p, of the multiple linear regression model are reported. The CP volume, LV volume, T_1, T_2, or MD exhibited significant positive correlations with WC.

found that serum leptin was 318% higher in individuals with obesity compared to lean participants. However, leptin concentration in the CSF of individuals with obesity was found to be only 30% higher than lean participants, which means a higher leptin CSF/serum ratio in lean participants (71). As mentioned previously, one of the roles of leptin is regulation of immune function. Leptin mediates recruitment of neutrophils at barrier structures, like the CP, involved in transporting immune cells into the brain (72). The increase in circulating leptin and, consequently, inflammation may serve as a potential explanation for the positive association since imaging studies on multiple sclerosis and depression have suggested a link between an increase in CNS inflammation and an enlarged CP (31, 73). However, the finding that BMI and WC did not have as a strong of an effect as age on CP volume suggests that they may not

be as strong of an indicator for obesity-related changes in volume. Studies examining associations in obesity-induced inflammation and CP volume are encouraged.

Further, we found that the LV volume was significantly larger in individuals with obesity compared to lean participants when using WC to distinguish between groups. Additionally, WC was found to have a significant positive relationship with LV volume. This finding is consistent with previous studies with a larger patient population of individuals that found a significant association between BMI or WC and LV volume (36, 74).

Of note, BMI was not sensitive enough to capture the differences between obese and lean groups in our study. Besides differences in the number of subjects per group due to the BMI or WC stratifications, the BMI is not a robust surrogate

TABLE 3 Slope, β, and significance, p, of the regression terms incorporated in the multiple linear regression given by: Lateral ventricle (LV) volume/intracranial volume (ICV), T_1, T_2, or mean diffusivity (MD) $\sim \beta_0 + \beta_{WC} \times WC + \beta_{age} \times age + \beta_{age}^2 \times age^2 + \beta_{sex} \times sex + \beta_{ethnicity} \times ethnicity$.

	Age		Age^2		Sex		Ethnicity		WC	
	β_{age}	p_{age}	β_{age}^2	p_{age}^2	β_{sex}	p_{sex}	$\beta_{ethnicity}$	$p_{ethnicity}$	β_{WC}	p_{WC}
CP volume/ICV	7.79×10^{-6}	**8.45×10^{-7}**	-7.06×10^{-8}	0.33	1.40×10^{-4}	**8.39×10^{-3}**	-2.58×10^{-5}	0.72	-4.19×10^{-6}	0.12
LV volume/ICV	3.30×10^{-4}	**4.86×10^{-12}**	9.84×10^{-6}	**6.86×10^{-5}**	-1.65×10^{-3}	0.37	-1.73×10^{-3}	0.49	2.10×10^{-4}	**2.32×10^{-2}**
T_1	19.34	**6.12×10^{-15}**	0.54	**1.65×10^{-5}**	-45.87	0.63	-63.61	0.65	8.06	**0.06**
T_2	2.08	**3.65×10^{-21}**	9.32×10^{-3}	0.35	-2.96	0.71	-16.68	0.15	0.09	0.81
MD	1.11×10^{-5}	**7.12×10^{-19}**	1.63×10^{-7}	**4.03×10^{-3}**	8.58×10^{-5}	**0.05**	-2.48×10^{-7}	0.99	1.88×10^{-6}	0.39

For the choroid plexus (CP) volume, multiple linear regression model was given by CP volume/ICV $\sim \beta_0 + \beta_{WC} \times WC + \beta_{age} \times age + \beta_{age}^2 \times age^2 + \beta_{sex} \times sex + \beta_{ethnicity} \times ethnicity + \beta_{LV} \times LV$. Sex and ethnicity results are not shown for associations with CP volume, LV volume, T_1, T_2, or MD. Bold indicates significance ($p < 0.05$) or close to significance ($p < 0.1$).

TABLE 4 Demographic characteristics of each group stratified using the established body mass index (BMI) cutoff points for lean participants (BMI < 25), overweight participants (25 $\leq$ BMI < 30), and participants with obesity (BMI $\geq$ 30) or using the established waist circumference (WC) cutoff points for lean participants (WC < 94 cm for men and WC < 80 cm for women), overweight participants (94 $\leq$ WC < 102 for men and 80 $\leq$ WC < 88 for women), and participants with obesity (WC $\geq$ 102 for men and WC $\geq$ 88 for women).

	BMI			WC			
	n (M, W)	MMSE Mean ± SD	BMI (kg/m^2) Mean ± SD	n (M, W)	MMSE Mean ± SD	Men (cm) Mean ± SD	Women (cm) Mean ± SD
Lean	56 (25, 31)	28.73 ± 1.52	22.56 ± 1.52	71 (41,30)	28.76 ± 1.42	86.17 ± 4.62	73.68 ± 4.68
Overweight	50 (32, 18)	28.85 ± 1.20	27.00 ± 1.15	31 (15,16)	28.93 ± 1.31	96.58 ± 2.72	84.10 ± 2.19
Obese	17 (8, 9)	28.59 ± 2.09	32.22 ± 1.91	21 (9,12)	28.52 ± 1.94	105.38 ± 2.74	95.92 ± 7.54

SD, standard deviation; MMSE, Mini-Mental State Examination; BMI, body-mass index; WC, waist circumference; M, Men; W, Women.

for body fat mass, while high BMI does not necessarily result in a higher mortality (75, 76). In contrast, WC provides higher predictive power of disease risk than does BMI (77, 78). Indeed, increased WC correlated better with increased insulin resistance, cancer and dyslipidemia than does BMI due to its strong association with the amount of visceral fat (58, 79, 80). However, it has been shown that increased WC in men corresponds to increases visceral fat whereas in women tends to be more related to subcutaneous fat (81). Excess visceral fat is associated with more adverse cardio-metabolic side effects compared to excess subcutaneous fat, thus these factors could

have independent effects on the outcomes in this. Further studies using DEXA scanning, the current gold-standard for determining regional body composition, are still required.

Although we examined a relatively large cohort and used advanced MR methodology, our study has limitations. Our dataset is cross-sectional so that the observed trends in the CP microstructure or volume with BMI or WC require further validation through longitudinal studies. Such work, motivated by the present results, is underway. Furthermore, our analysis of functional and structural differences in CP with aging were limited to the LVs. We note that CSF partial volume effects
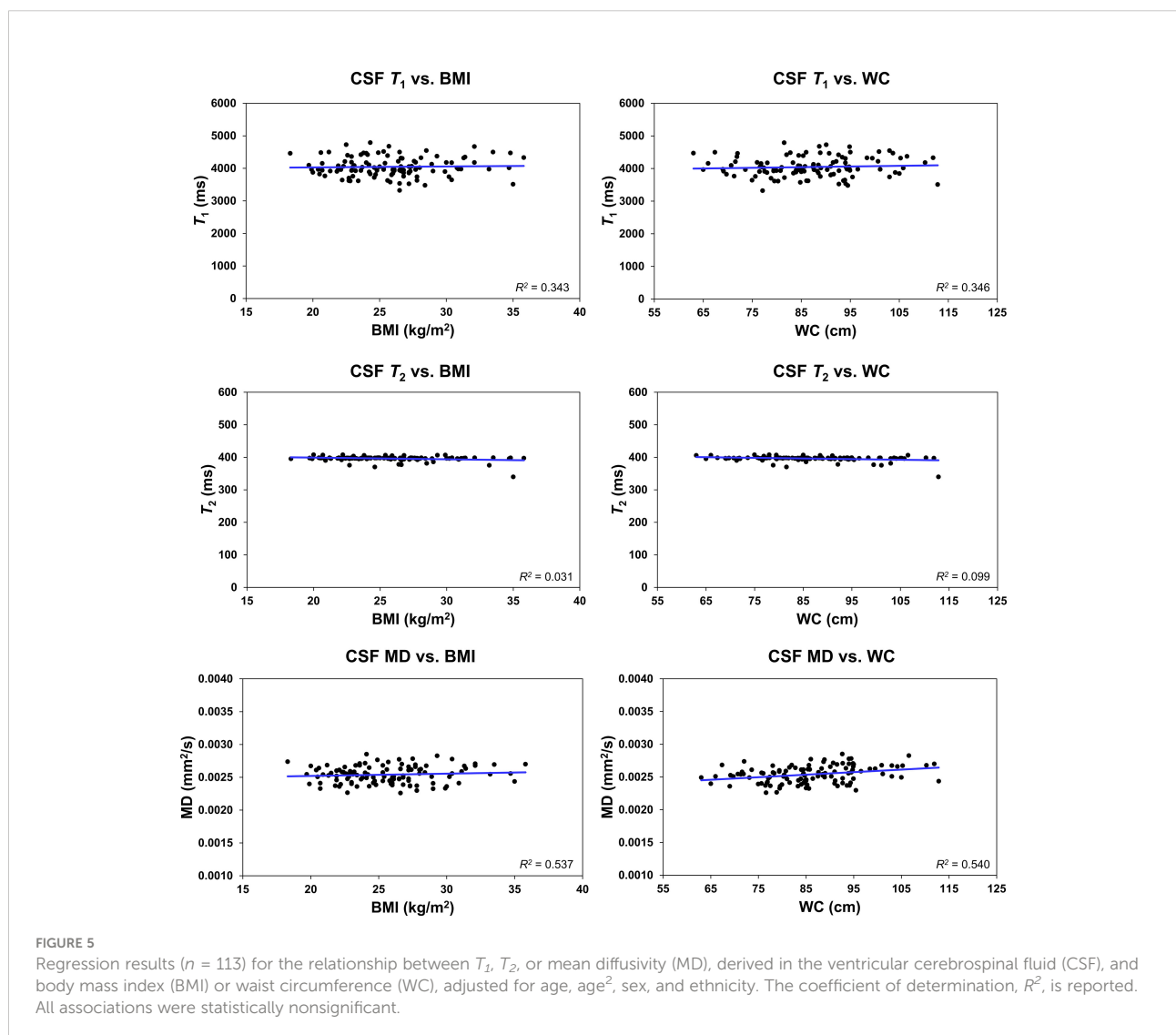
TABLE 5 Significance, p-value, of the between-group ANCOVA analyses of the effect of body mass index (BMI) or waist circumference (WC) on lateral ventricle (LV) volume/intracranial volume (ICV), T_1, T_2, or mean diffusivity (MD).

	Obese vs. Lean		Overweight vs. Lean		Obese vs. Overweight	
	BMI	WC	BMI	WC	BMI	WC
CP volume/ICV	0.18	0.33	0.26	0.12	0.91	0.51
LV volume/ICV	**0.03**	**8.90×10^{-3}**	0.76	0.34	0.45	0.39
T_1	0.12	**0.04**	0.37	0.48	**0.03**	0.54
T_2	0.49	0.38	0.11	0.63	0.11	0.71
MD	0.39	**0.07**	0.12	0.73	**0.03**	0.75

All between-group comparisons were controlled for age, age^2, sex, and ethnicity. For CP volume/ICV, between-group comparisons were controlled for age, age^2, sex, ethnicity, and LV volume. Bold indicates significance ($p < 0.05$) or close to significance ($p < 0.1$).

TABLE 6   Mean and standard deviation (SD) values of each magnetic resonance imaging (MRI) metric. Each group was stratified using the established body mass index (BMI) cutoff points for lean participants (BMI < 25), overweight participants (25 ≤ BMI < 30), and participants with obesity (BMI ≥ 30) or using the established waist circumference (WC) cutoff points for lean participants (WC < 94 cm for men and WC < 80 cm for women), overweight participants (94 ≤ WC < 102 for men and 80 ≤ WC < 88 for women), and participants with obesity (WC ≥ 102 for men and WC ≥ 88 for women).

	BMI			WC		
	Lean	**Overweight**	**Obese**	**Lean**	**Overweight**	**Obese**
CP volume/ICV (10^{-3})	1.06 ± 0.35	1.06 ± 0.51	1.17 ± 0.57	1.01 ± 0.38	1.07 ± 0.46	1.31 ± 0.58
LV volume/ICV (10^{-3})	18.81 ± 8.85	19.94 ± 15.0	24.73 ± 13.6	17.33 ± 8.95	21.34 ± 14.35	27.56 ± 16.18
T_1 (ms)	2605 ± 614	2526 ± 665	2882 ± 696	2512 ± 604	2601 ± 687	2937 ± 674
T_2 (ms)	319 ± 54	309 ± 59	333 ± 57	309 ± 56	315 ± 63	346 ± 40
MD (mm^2/s) (10^{-3})	2.08 ± 0.32	2.06 ± 0.36	2.18 ± 0.31	2.03 ± 0.33	2.11 ± 0.37	2.26 ± 0.26

FIGURE 5
Regression results (n = 113) for the relationship between T_1, T_2, or mean diffusivity (MD), derived in the ventricular cerebrospinal fluid (CSF), and body mass index (BMI) or waist circumference (WC), adjusted for age, age^2, sex, and ethnicity. The coefficient of determination, R^2, is reported. All associations were statistically nonsignificant.

may bias derived parameter values (82). However, our analysis indicates that the observed trends of the MR parameters are driven by differences in the CP's microstructure as all parameters derived in the CSF exhibited nonsignificant associations with BMI or WC. Nevertheless, more accurate automated segmentation methods, including the third and fourth ventricles, as well as higher resolution structural images are needed for a better evaluation. In addition, our DTI-related results must be interpreted with caution. Indeed, given the large fraction of free water in the CP, this could have introduced bias in derived parameter values. Although the free-water elimination DTI (FWE-DTI) approach has been used widely to distinguish free-water partial-volume effects from tissue's diffusion in healthy aging and degenerative diseases (83), it has recently been shown that this method is unstable when applied to single-shell DTI data, requiring careful implementation (84). In line with the FEW-DTI approach, a bicomponent relaxometry approach could, in principle, be used to correct for the potential contamination due to CSF in derived T_1 and T_2. This model my incorporate a parenchymal compartment and a CSF compartment. However, such approach will require extensive validation and testing which is out of the scope of this work but represents one of the future directions in our CP-related investigations. Further, we note that our derived DTI parameters values could change depending on the choice of the b-values. Several DTI protocols involve use of b-values of 0 and 1000 s/mm^2 while others incorporate lower b-values. Finally, other factors such as inflammatory markers, diet, and medications were not considered in this work. Indeed, obesity is associated with a plethora of metabolic consequences such as hyperglycemia, insulin resistance and dyslipidemia, while it has recently been shown that the CP is a site of insulin secretion (85). Therefore, the CP may be directly influenced by the state of obesity and the fluid movement differences identified here.

In conclusion, we examined associations between obesity and CP microstructure in a large cohort and across a wide age range of cognitively unimpaired participants. Obesity may represent a modifiable risk factor for disruption of CP structure, and therefore an important therapeutic target. Our results indicate the possibility of a link between obesity and CP structure and volume, and therefore provide a foundation for further investigation of, for example, the effect of diet and physical activity on CP microstructure and function.

Data availability statement

The raw data supporting the conclusions of this article will be made available by the authors, without undue reservation.

Ethics statement

The MRI protocol was approved by the MedStar Research Institute and the National Institutes of Health Intramural Ethics Committees, and all examinations were performed in compliance with the standards established by the National Institutes of Health Institutional Review Board. The patients/participants provided their written informed consent to participate in this study.

Author contributions

Funding

Acknowledgments

Conflict of interest

The authors declare that the research was conducted in the absence of any commercial or financial relationships that could be construed as a potential conflict of interest.

Publisher's note

All claims expressed in this article are solely those of the authors and do not necessarily represent those of their affiliated organizations, or those of the publisher, the editors and the reviewers. Any product that may be evaluated in this article, or claim that may be made by its manufacturer, is not guaranteed or endorsed by the publisher.

References

1. Chooi YC, Ding C, Magkos F. The epidemiology of obesity. *Metabolism* (2019) 92:6–10. doi: 10.1016/j.metabol.2018.09.005

2. Pi-Sunyer X. The medical risks of obesity. *Postgrad Med* (2009) 121(6):21–33. doi: 10.3810/pgm.2009.11.2074

3. Alford S, Patel D, Perakakis N, Mantzoros CS. Obesity as a risk factor for alzheimer's disease: Weighing the evidence. *Obes Rev* (2018) 19(2):269–80. doi: 10.1111/obr.12629

4. Mazon JN, de Mello AH, Ferreira GK, Rezin GT. The impact of obesity on neurodegenerative diseases. *Life Sci* (2017) 182:22–8. doi: 10.1016/j.lfs.2017.06.002

5. Novo AM, Batista S. Multiple sclerosis: Implications of obesity in neuroinflammation. *Adv Neurobiol* (2017) 19:191–210. doi: 10.1007/978-3-319-63260-5_8

6. Hedström AK, Lima Bomfim I, Barcellos L, Gianfrancesco M, Schaefer C, Kockum I, et al. Interaction between adolescent obesity and hla risk genes in the etiology of multiple sclerosis. *Neurology* (2014) 82(10):865. doi: 10.1212/WNL.0000000000000203

7. Bouhrara M, Khattar N, Elango P, Resnick SM, Ferrucci L, Spencer RG. Evidence of association between obesity and lower cerebral myelin content in cognitively unimpaired adults. *Int J Obes (Lond)* (2021) 45(4):850–9. doi: 10.1038/s41366-021-00749-x

8. Marques-Iturria I, Pueyo R, Garolera M, Segura B, Junque C, Garcia-Garcia I, et al. Frontal cortical thinning and subcortical volume reductions in early adulthood obesity. *Psychiatry Res* (2013) 214(2):109–15. doi: 10.1016/j.pscychresns.2013.06.004

9. Debette S, Wolf C, Lambert JC, Crivello F, Soumare A, Zhu YC, et al. Abdominal obesity and lower Gray matter volume: A mendelian randomization study. *Neurobiol Aging* (2014) 35(2):378–86. doi: 10.1016/j.neurobiolaging.2013.07.022

10. Peng SL, Chen CM. The influence of obesity on cerebral blood flow in young adults using arterial spin labeling mri. *NMR BioMed* (2020) 33(10):e4375. doi: 10.1002/nbm.4375

11. Ashrafian H, Harling L, Darzi A, Athanasiou T. Neurodegenerative disease and obesity: What is the role of weight loss and bariatric interventions? *Metab Brain Dis* (2013) 28(3):341–53. doi: 10.1007/s11011-013-9412-4

12. Liu Y, Yan T, Chu JM, Chen Y, Dunnett S, Ho YS, et al. The beneficial effects of physical exercise in the brain and related pathophysiological mechanisms in neurodegenerative diseases. *Lab Invest* (2019) 99(7):943–57. doi: 10.1038/s41374-019-0232-y

13. Balusu S, Van Wonterghem E, De Rycke R, Raemdonck K, Stremersch S, Gevaert K, et al. Identification of a novel mechanism of blood-brain communication during peripheral inflammation *via* choroid plexus-derived extracellular vesicles. *EMBO Mol Med* (2016) 8(10):1162–83. doi: 10.15252/emmm.201606271

14. Kanoski SE, Zhang Y, Zheng W, Davidson TL. The effects of a high-energy diet on hippocampal function and blood-brain barrier integrity in the rat. *J Alzheimers Dis* (2010) 21(1):207–19. doi: 10.3233/JAD-2010-091414

15. Guillemot-Legris O, Muccioli GG. Obesity-induced neuroinflammation: Beyond the hypothalamus. *Trends Neurosci* (2017) 40(4):237–53. doi: 10.1016/j.tins.2017.02.005

16. Lun MP, Monuki ES, Lehtinen MK. Development and functions of the choroid plexus-cerebrospinal fluid system. *Nat Rev Neurosci* (2015) 16(8):445–57. doi: 10.1038/nrn3921

17. Arnaud K, Di Nardo AA. Choroid plexus trophic factors in the developing and adult brain. *Front Biol* (2016) 11(3):214–21. doi: 10.1007/s11515-016-1401-7

18. Marques F, Sousa JC, Sousa N, Palha JA. Blood–Brain-Barriers in aging and in alzheimer's disease. *Mol Neurodegen* (2013) 8(1):38. doi: 10.1186/1750-1326-8-38

19. Nestor SM, Rupsingh R, Borrie M, Smith M, Accomazzi V, Wells JL, et al. Ventricular enlargement as a possible measure of alzheimer's disease progression validated using the alzheimer's disease neuroimaging initiative database. *Brain* (2008) 131(Pt 9):2443–54. doi: 10.1093/brain/awn146

20. Serot J-M, Béné M-C, Foliguet B, Faure GC. Morphological alterations of the choroid plexus in late-onset alzheimer's disease. *Acta Neuropathol* (2000) 99 (2):105–8. doi: 10.1007/PL00007412

21. Vercellino M, Votta B, Condello C, Piacentino C, Romagnolo A, Merola A, et al. Involvement of the choroid plexus in multiple sclerosis autoimmune inflammation: A neuropathological study. *J Neuroimmunol* (2008) 199(1-2):133–41. doi: 10.1016/j.jneuroim.2008.04.035

22. Turner B, Ramli N, Blumhardt LD, Jaspan T. Ventricular enlargement in multiple sclerosis: A comparison of three-dimensional and linear mri estimates. *Neuroradiology* (2001) 43(8):608–14. doi: 10.1007/s002340000457

23. Simon JH, Jacobs LD, Campion MK, Rudick RA, Cookfair DL, Herndon RM, et al. A longitudinal study of brain atrophy in relapsing multiple sclerosis. *Neurology* (1999) 53(1):139. doi: 10.1212/WNL.53.1.139

24. Kalyan-Masih P, Vega-Torres JD, Miles C, Haddad E, Rainsbury S, Baghchechi M, et al. Western High-fat diet consumption during adolescence increases susceptibility to traumatic stress while selectively disrupting hippocampal and ventricular volumes. *eNeuro* (2016) 3(5):1–24. doi: 10.1523/ENEURO.0125-16.2016

25. Schreurs BG, Smith-Bell CA, Lemieux SK. Dietary cholesterol increases ventricular volume and narrows cerebrovascular diameter in a rabbit model of alzheimer's disease. *Neuroscience* (2013) 254:61–9. doi: 10.1016/j.neuroscience.2013.09.015

26. Hubert V, Chauveau F, Dumot C, Ong E, Berner LP, Canet-Soulas E, et al. Clinical imaging of choroid plexus in health and in brain disorders: A mini-review. *Front Mol Neurosci* (2019) 12:34. doi: 10.3389/fnmol.2019.00034

27. Alicioglu B, Yilmaz G, Tosun O, Bulakbasi N. Diffusion-weighted magnetic resonance imaging in the assessment of choroid plexus aging. *Neuroradiol J* (2017) 30(5):490–5. doi: 10.1177/1971400917714280

28. Alisch JSR, Kiely M, Triebswetter C, Alsameen MH, Gong Z, Khattar N, et al. Characterization of age-related differences in the human choroid plexus volume, microstructural integrity, and blood perfusion using multiparameter magnetic resonance imaging. *Front Aging Neurosci* (2021) 13:734992. doi: 10.3389/fnagi.2021.734992

29. Zhou G, Hotta J, Lehtinen MK, Forss N, Hari R. Enlargement of choroid plexus in complex regional pain syndrome. *Sci Rep* (2015) 5:14329. doi: 10.1038/srep14329

30. Egorova N, Gottlieb E, Khlif MS, Spratt NJ, Brodtmann A. Choroid plexus volume after stroke. *Int J Stroke* (2019) 14(9):923–30. doi: 10.1177/1747493019851277

31. Ricigliano VAG, Morena E, Colombi A, Tonietto M, Hamzaoui M, Poirion E, et al. Choroid plexus enlargement in inflammatory multiple sclerosis: 3.0-T mri and translocator protein pet evaluation. *Radiology* (2021) 301(1):166–77. doi: 10.1148/radiol.2021204426

32. Lizano P, Lutz O, Ling G, Lee AM, Eum S, Bishop JR, et al. Association of choroid plexus enlargement with cognitive, inflammatory, and structural phenotypes across the psychosis spectrum. *Am J Psychiatry* (2019) 176(7):564–72. doi: 10.1176/appi.ajp.2019.18070825

33. Deoni SC. Quantitative relaxometry of the brain. *Top Magn Reson Imaging* (2010) 21(2):101–13. doi: 10.1097/RMR.0b013e31821e56d8

34. Grech-Sollars M, Hales PW, Miyazaki K, Raschke F, Rodriguez D, Wilson M, et al. Multi-centre reproducibility of diffusion mri parameters for clinical sequences in the brain. *NMR BioMed* (2015) 28(4):468–85. doi: 10.1002/nbm.3269

35. Alexander AL, Lee JE, Lazar M, Field AS. Diffusion tensor imaging of the brain. *Neurotherapeutics* (2007) 4(3):316–29. doi: 10.1016/j.nurt.2007.05.011

36. Ho AJ, Raji CA, Becker JT, Lopez OL, Kuller LH, Hua X, et al. Obesity is linked with lower brain volume in 700 ad and mci patients. *Neurobiol Aging* (2010) 31(8):1326–39. doi: 10.1016/j.neurobiolaging.2010.04.006

37. Zhou YF, Huang JC, Zhang P, Fan FM, Chen S, Fan HZ, et al. Choroid plexus enlargement and allostatic load in schizophrenia. *Schizophr Bull* (2020) 46 (3):722–31. doi: 10.1093/schbul/sbz100

38. Suvarna B, Suvarna A, Phillips R, Juster RP, McDermott B, Sarnyai Z. Health risk behaviours and allostatic load: A systematic review. *Neurosci Biobehav Rev* (2020) 108:694–711. doi: 10.1016/j.neubiorev.2019.12.020

39. Ferrucci L. The Baltimore longitudinal study of aging (Blsa): A 50-Year-Long journey and plans for the future. *journals gerontol Ser A Biol Sci Med Sci* (2008) 63(12):1416. doi: 10.1093/gerona/63.12.1416

40. Shock NW. *Normal human aging: The Baltimore longitudinal study of aging*. Shock NW, editor. Baltimore, Md: U.S. Dept. of Health and Human Services, Public Health Service, National Institutes of Health, National Institute on Aging, Gerontology Research Center (1984).

41. O'Brien RJ, Resnick SM, Zonderman AB, Ferrucci L, Crain BJ, Pletnikova O, et al. Neuropathologic studies of the Baltimore longitudinal study of aging (Blsa). *J Alzheimer's Dis JAD* (2009) 18(3):665–75. doi: 10.3233/JAD-2009-1179

42. Bouhrara M, Reiter DA, Celik H, Fishbein KW, Kijowski R, Spencer RG. Analysis of mcdespot- and cpmg-derived parameter estimates for two-component nonexchanging systems. *Magn Reson Med* (2016) 75(6):2406–20. doi: 10.1002/mrm.25801

43. Bouhrara M, Spencer RG. Incorporation of nonzero echo times in the spgr and bssfp signal models used in mcdespot. *Magn Reson Med* (2015) 74(5):1227–35. doi: 10.1002/mrm.25984

44. Bouhrara M, Spencer RG. Improved determination of the myelin water fraction in human brain using magnetic resonance imaging through Bayesian analysis of mcdespot. *Neuroimage* (2016) 127:456–71. doi: 10.1016/j.neuroimage.2015.10.034

45. Bouhrara M, Spencer RG. Rapid simultaneous high-resolution mapping of myelin water fraction and relaxation times in human brain using bmc-mcdespot. *Neuroimage* (2017) 147:800–11. doi: 10.1016/j.neuroimage.2016.09.064

46. Stollberger R, Wach P. Imaging of the active B1 field *in vivo*. *Magnetic Resonance Med* (1996) 35(2):246–51. doi: 10.1002/mrm.1910350217

47. Fischl B, Salat DH, Busa E, Albert M, Dieterich M, Haselgrove C, et al. Whole brain segmentation: Automated labeling of neuroanatomical structures in the human brain. *Neuron* (2002) 33(3):341–55. doi: 10.1016/S0896-6273(02)00569-X

48. Fischl B. Freesurfer. *Neuroimage* (2012) 62(2):774–81. doi: 10.1016/j.neuroimage.2012.01.021

49. Chaddad A, Desrosiers C, Toews M. Multi-scale radiomic analysis of Sub-cortical regions in mri related to autism, gender and age. *Sci Rep* (2017) 7:45639. doi: 10.1038/srep45639

50. Tadayon E, Pascual-Leone A, Press D, Santarnecchi E. Alzheimer's disease neuroimaging i. choroid plexus volume is associated with levels of csf proteins: Relevance for alzheimer's and parkinson's disease. *Neurobiol Aging* (2020) 89:108–17. doi: 10.1016/j.neurobiolaging.2020.01.005

51. Jenkinson M, Beckmann CF, Behrens TE, Woolrich MW, Smith SM. Fsl. *Neuroimage* (2012) 62(2):782–90. doi: 10.1016/j.neuroimage.2011.09.015

52. Deoni SC, Rutt BK, Peters TM. Rapid combined T1 and T2 mapping using gradient recalled acquisition in the steady state. *Magn Reson Med* (2003) 49(3):515–26. doi: 10.1002/mrm.10407

53. Berger MF, Silverman HF. Microphone array optimization by stochastic region contraction. *Signal Processing IEEE Trans* (1991) 39(11):2377–86. doi: 10.1109/78.97993

54. Basser PJ, Jones DK. Diffusion-tensor mri: Theory, experimental design and data analysis - a technical review. *NMR biomed* (2002) 15(7-8):456–67. doi: 10.1002/nbm.783

55. Bouhrara M, Rejimon AC, Cortina LE, Khattar N, Bergeron CM, Ferrucci L, et al. Adult brain aging investigated using bmc-Mcdespot-Based myelin water fraction imaging. *Neurobiol Aging* (2020) 85:131–9. doi: 10.1016/j.neurobiolaging.2019.10.003

56. Arshad M, Stanley JA, Raz N. Adult age differences in subcortical myelin content are consistent with protracted myelination and unrelated to diffusion tensor imaging indices. *Neuroimage* (2016) 143:26–39. doi: 10.1016/j.neuroimage.2016.08.047

57. Zhang Y, Brady M, Smith S. Segmentation of brain Mr images through a hidden Markov random field model and the expectation-maximization algorithm. *IEEE Trans Med Imaging* (2001) 20(1):45–57. doi: 10.1109/42.906424

58. Janssen I, Katzmarzyk PT, Ross R. Body mass index, waist circumference, and health risk: Evidence in support of current national institutes of health guidelines. *Arch Internal Med* (2002) 162(18):2074–9. doi: 10.1001/archinte.162.18.2074

59. Salat DH. Chapter 12 - diffusion tensor imaging in the study of aging and age-associated neural disease. In: Johansen-Berg H, Behrens TEJ, editors. *Diffusion mri (Second edition)*. San Diego: Academic Press (2014). p. 257–81.

60. Sainz N, Barrenetxe J, Moreno-Aliaga MJ, Martinez JA. Leptin resistance and diet-induced obesity: Central and peripheral actions of leptin. *Metabolism* (2015) 64(1):35–46. doi: 10.1016/j.metabol.2014.10.015

61. Mantzoros CS, Magkos F, Brinkoetter M, Sienkiewicz E, Dardeno TA, Kim SY, et al. Leptin in human physiology and pathophysiology. *Am J Physiol Endocrinol Metab* (2011) 301(4):E567–84. doi: 10.1152/ajpendo.00315.2011

62. Tartaglia LA. The leptin receptor. *J Biol Chem* (1997) 272(10):6093–6. doi: 10.1074/jbc.272.10.6093

63. Dietrich MO, Spuch C, Antequera D, Rodal I, de Yebenes JG, Molina JA, et al. Megalin mediates the transport of leptin across the blood-csf barrier. *Neurobiol Aging* (2008) 29(6):902–12. doi: 10.1016/j.neurobiolaging.2007.01.008

64. Merino B, Diez-Fernandez C, Ruiz-Gayo M, Somoza B. Choroid plexus epithelial cells Co-express the long and short form of the leptin receptor. *Neurosci Lett* (2006) 393(2-3):269–72. doi: 10.1016/j.neulet.2005.10.003

65. Hayden MR, Banks WA. Deficient leptin cellular signaling plays a key role in brain ultrastructural remodeling in obesity and type 2 diabetes mellitus. *Int J Mol Sci* (2021) 22(11)1–22. doi: 10.3390/ijms22115427

66. Castellazzi M, Morotti A, Tamborino C, Alessi F, Pilotto S, Baldi E, et al. Increased age and Male sex are independently associated with higher frequency of blood-cerebrospinal fluid barrier dysfunction using the albumin quotient. *Fluids Barriers CNS* (2020) 17(1):14. doi: 10.1186/s12987-020-0173-2

67. Seyfert S, Kunzmann V, Schwertfeger N, Koch HC, Faulstich A. Determinants of lumbar csf protein concentration. *J Neurol* (2002) 249(8):1021–6. doi: 10.1007/s00415-002-0777-2

68. Wakerley BR, Warner R, Cole M, Stone K, Foy C, Sittampalam M. Cerebrospinal fluid opening pressure: The effect of body mass index and body composition. *Clin Neurol Neurosurg* (2020) 188:105597. doi: 10.1016/j.clineuro.2019.105597

69. Uldall M, Bhatt DK, Kruuse C, Juhler M, Jansen-Olesen I, Jensen RH. Choroid plexus aquaporin 1 and intracranial pressure are increased in obese rats: Towards an idiopathic intracranial hypertension model? *Int J Obes* (2017) 41(7):1141–7. doi: 10.1038/ijo.2017.83

70. Choi JD, Moon Y, Kim HJ, Yim Y, Lee S, Moon WJ. Choroid plexus volume and permeability at brain mri within the Alzheimer disease clinical spectrum. *Radiology* (2022) 304:635–45. doi: 10.1148/radiol.212400

71. Caro JF, Kolaczynski JW, Nyce MR, Ohannesian JP, Opentanova I, Goldman WH, et al. Decreased cerebrospinal-Fluid/Serum leptin ratio in obesity: A possible mechanism for leptin resistance. *Lancet* (1996) 348(9021):159–61. doi: 10.1016/s0140-6736(96)03173-x

72. Rummel C, Inoue W, Poole S, Luheshi GN. Leptin regulates leukocyte recruitment into the brain following systemic lps-induced inflammation. *Mol Psychiatry* (2010) 15(5):523–34. doi: 10.1038/mp.2009.98

73. Althubaity N, Schubert J, Martins D, Yousaf T, Nettis MA, Mondelli V, et al. Choroid plexus enlargement is associated with neuroinflammation and reduction of blood brain barrier permeability in depression. *NeuroImage Clin* (2022) 33:102926. doi: 10.1016/j.nicl.2021.102926

74. McWhinney SR, Abe C, Alda M, Benedetti F, Boen E, Del Mar Bonnin C, et al. Association between body mass index and subcortical brain volumes in bipolar disorders-enigma study in 2735 individuals. *Mol Psychiatry* (2021) 26(11):6806–19. doi: 10.1038/s41380-021-01098-x

75. Flegal KM, Kit BK, Orpana H, Graubard BI. Association of all-cause mortality with overweight and obesity using standard body mass index categories: A systematic review and meta-analysis. *JAMA* (2013) 309(1):71–82. doi: 10.1001/jama.2012.113905

76. Winter JE, MacInnis RJ, Wattanapenpaiboon N, Nowson CA. Bmi and all-cause mortality in older adults: A meta-analysis. *Am J Clin Nutr* (2014) 99(4):875–90. doi: 10.3945/ajcn.113.068122

77. Staiano AE, Reeder BA, Elliott S, Joffres MR, Pahwa P, Kirkland SA, et al. Body mass index versus waist circumference as predictors of mortality in Canadian adults. *Int J Obes* (2012) 36(11):1450–4. doi: 10.1038/ijo.2011.268

78. Janssen I, Katzmarzyk PT, Ross R. Waist circumference and not body mass index explains obesity-related health risk. *Am J Clin Nutr* (2004) 79(3):379–84. doi: 10.1093/ajcn/79.3.379

79. Kuk JL, Katzmarzyk PT, Nichaman MZ, Church TS, Blair SN, Ross R. Visceral fat is an independent predictor of all-cause mortality in men. *Obesity* (2006) 14(2):336–41. doi: 10.1038/oby.2006.43

80. Calle EE, Kaaks R. Overweight, obesity and cancer: Epidemiological evidence and proposed mechanisms. *Nat Rev Cancer* (2004) 4(8):579–91. doi: 10.1038/nrc1408

81. Staynor JMD, Smith MK, Donnelly CJ, Sallam AE, Ackland TR. Dxa reference values and anthropometric screening for visceral obesity in Western Australian adults. *Sci Rep* (2020) 10(1):18731. doi: 10.1038/s41598-020-73631-x

82. Lee H, Ozturk B, Stringer MS, Koundal S, MacIntosh BJ, Rothman D, et al. Choroid plexus tissue perfusion and blood to csf barrier function in rats measured with continuous arterial spin labeling. *NeuroImage* (2022) 261:119512. doi: 10.1016/j.neuroimage.2022.119512

83. Pasternak O, Sochen N, Gur Y, Intrator N, Assaf Y. Free water elimination and mapping from diffusion mri. *Magn Reson Med* (2009) 62(3):717–30. doi: 10.1002/mrm.22055

84. Golub M, Neto Henriques R, Gouveia Nunes R. Free-water dti estimates from single b-value data might seem plausible but must be interpreted with care. *Magn Reson Med* (2021) 85(5):2537–51. doi: 10.1002/mrm.28599

85. Mazucanti CH, Liu QR, Lang D, Huang N, O'Connell JF, Camandola S, et al. Release of insulin produced by the choroid plexis is regulated by serotonergic signaling. *JCI Insight* (2019) 4(23):e131682. doi: 10.1172/jci.insight.131682